Marine Geodesy, 23:145–166, 2000

0149-0419/00 $12.00 + .00

An Improved Calibration of Satellite Altimetric Heights Using Tide Gauge Sea Levels with Adjustment for Land Motion

GARY T. MITCHUM

Department of Marine Science
University of South Florida
St. Petersburg, FL

Several major improvements to an existing method for calibrating satellite altimeters using tide gauge data are described. The calibration is in the sense of monitoring and correcting temporal drift in the altimetric time series, which is essential in efforts to use the altimetric data for especially demanding applications. Examples include the determination of the rate of change of global mean sea level and the study of the relatively subtle, but climatically important, decadal variations in basin scale sea levels. The improvements are to the method described by Mitchum (1998a), and the modifications are of two basic types. First, since the method depends on the cancellation of true ocean signals by differencing the altimetric data from the tide gauge sea level time series, improvements are made that produce a more complete removal of the ocean signals that comprise the noise for the altimetric drift estimation problem. Second, a major error source in the tide gauge data, namely land motion, is explicitly addressed and corrections are developed that incorporate space-based geodetic data (continuous GPS and DORIS measurements). The long-term solution, having such geodetic measurements available at all the tide gauges, is not yet a reality, so an interim solution is developed. The improved method is applied to the TOPEX altimetric data. The Side A data (August 1992–February 1999) are found to have a linear drift component of −0.55 +/− 0.39 mm/yr, but there is also a significant quadratic component to the drift that is presently unexplained. The TOPEX Side B altimeter is estimated to be biased by 7.0 +/− 0.7 mm relative to the Side A altimeter based on an analysis of the first 350 days of Side B data.

Keywords satellite altimetry, sea level variations, tide gauges, instruments and methods

In the past decade satellite altimetry has become a valuable tool in several areas of geophysics, including oceanography and geodesy, and the interested reader is referred to various review articles for more information. For example, Fu (2000) and Wunsch and Stammer (1998) review studies of ocean and climate variability, and a wide variety of topics in geophysics are covered in a special issue of the *Journal of Geophysical Research—Oceans* (JGR 1995) devoted to geophysical studies that use data from the TOPEX/Poseidon (T/P)

The author would like to thank many colleagues for helpful conversations during the course of this work, including S. Nerem, D. Chambers, A. Cazenave, J.-F. Cretaux, B. Haines, and G. Hayne. Sea level data were provided by the University of Hawaii Sea Level Center and the Permanent Service for Mean Sea Level. GPS and DORIS data were provided by M. Watkins, A. Cazenave and J.-F. Cretaux. This work was supported by NASA through the Jet Propulsion Laboratory as part of the TOPEX Altimeter Research in Ocean Circulation Mission and the JASON-1 Project.

Address correspondence to: Gary T. Mitchum, Dept. of Marine Science, Univ. of South Florida, 140 Seventh Avenue, St. Petersburg, FL 33701. E-mail: mitchum@marine.usf.edu

altimetry mission. We will take it as given that the value of altimetry has been proven, especially in the case of the highly precise T/P data, which is the dataset that we will use throughout this article. Given the successes to date, these data will undoubtedly be used for more and more challenging problems in the future. For example, altimetry has been used since early in the T/P mission for the determination of global sea level change (e.g., Nerem 1995; Minster, Brossier and Rogel 1995; Nerem et al. 1997; Cazenave et al. 1998), and a summary of these calculations has been given by Nerem and Mitchum (2000). More recently, work concerning smaller amplitude interannual changes in the global mean sea level have been undertaken as well (Nerem et al. 1999). We also expect that the altimetric data will be applied to studies of decadal sea level variations as the time series lengthen, complementing existing studies that use long tide gauge records (e.g., Sturges, Hong and Clarke 1998; Hong, Sturges and Clarke 2000).

To enable such studies of low frequency, small amplitude signals, we must ensure that the altimetric time series are extremely stable. Mitchum (1998a; hereinafter M98) has addressed this problem and has shown an application to the TOPEX altimeter. In this study we also restrict our attention to the TOPEX data because of the relatively small quantity of Poseidon data in the total T/P dataset. The M98 study developed an analogy between the use of tide gauges to ensure altimetric stability and the use of tide staffs to ensure the stability of tide gauges, summarized various alternative approaches to the problem, and presented a method that uses a global set of tide gauge sea levels for altimetric drift estimation. In addition to looking for true sources of drift due to the instruments comprising the altimetric system, the M98 method can also be used to level the time series from different altimeters, or from different altimeters on the same satellite. Readers familiar with tide gauge operations will recognize this problem as analogous to that of maintaining the tide gauge datum when tide gauges are replaced, or when instruments are reinstalled after a hiatus in the observations.

The M98 method used a simple matching of the tide gauge series with the altimetric data from the nearest four altimeter passes in which the altimetric height series were sampled only at the single latitude where the tide gauge is located. Differences between the altimetric heights and the tide gauge sea levels were then computed, allowing the true ocean signals to cancel, thus leaving the altimeter drift error to dominate the difference series. The tide gauges were assumed to be vertically stable, but an estimate of the bias error due to this assumption was made. M98 carefully considered the statistics of, first, how to best combine the data from the four passes at a given tide gauge station, and second, how to best combine the data from the various tide gauges in the global set to obtain a time series of the estimated altimetric drift. Since the publication of M98, the method has been substantially improved, and describing these changes is the primary goal of this article. There have been three major changes that we will discuss here. First, additional tide gauge stations have been included. Second, better signal matching between the tide gauge and the nearby altimeter passes has been done in order to improve the signal to noise ratio in the differences. Third, and most important, a land motion correction has been made, which M98 identified as the area most needing improvement. We note also that M98 suggested a possible drift in the water vapor radiometer (TMR) measurement on T/P, a suggestion that was subsequently confirmed and corrected (Keihm et al. 1998). This correction has been incorporated into all of the TOPEX data that we use, and will not be discussed further in this article.

The article is organized as follows. It begins by detailing the improvements made to the basic method of M98. It then considers the land motion problem in detail and describes the present approach. Finally, it presents the most recent results from the TOPEX stability analysis.

Improvements to the Basic Method

The improvements to the basic M98 method include the use of more tide gauge stations, as well as more altimetry data at each station, and a better matching of the ocean signals common to the altimetric and tide gauge time series. The improved ocean signal matching results in a larger signal to noise ratio for the difference time series, in which the signal is the drift error that we want to study, and the noise is that portion of the true ocean signal that does not cancel perfectly when the altimeter and tide gauge time series are differenced. The treatment of the land motion errors will be taken up in the next section.

The basic strength of the global tide gauge approach to the altimeter calibration problem (M98) is that we have many more degrees of freedom than are available at specialized calibration sites, such as the T/P calibration site on the Harvest platform (Christensen et al. 1994), for example. M98 considered 101 tide gauge stations, and, after excluding stations where the tide gauge or altimetric time series were considered inadequate for some reason, 53 of these stations were used in the final analysis. We are now considering 132 stations (Figure 1), and find that 108 of these produce useful series. The 24 stations that were not used were rejected for a variety of reasons (Table 1). In eight cases the tide gauge, altimeter overlap period was considered to be too short (less than 2 years). In 11 cases problems appeared to exist with the land motion correction, which will be discussed below. In three cases the tide gauge record was considered questionable due to an apparent datum shift. In the two remaining cases the tide gauge and altimetric series did not correlate well, meaning that the signal cancellation that is the heart of the method cannot be expected to work. It is unfortunate that five of the 24 stations rejected are in the data sparse region south of 35°S. This is primarily due to short time series and difficulty with quality control, which highlights the need for additional in situ sea level measurements in the region.

There are two reasons why many more stations, 108 rather than 53, contribute to the present analysis. First, in addition to the near real-time stations that M98 considered, some delayed mode stations are now included. Since the altimetric time series are now almost a decade long, even tide gauges that are lacking the past year or two of data can still make

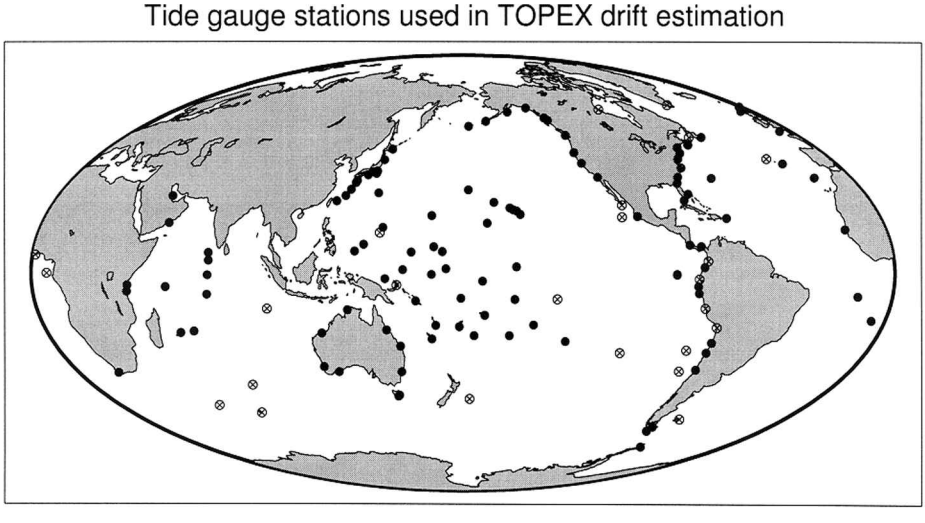

FIGURE 1 Sea level stations considered in this study. The solid circles are stations that were actually used, and the open circles with crosses are stations that were rejected during the quality control (see also Table 1). Daily sea level values are available at all stations.

TABLE 1 Tide Gauge Stations Rejected During Quality Control

Station name	N Lat	E Lon	Reason for rejection
Port Stanley	−51.75	−57.93	No reliable land motion estimate
Kerguelen	−49.34	70.22	Possible tide gauge level shift
Crozet	−46.42	51.87	Overlap data period too short
Chatham	−43.95	−176.56	Overlap data period too short
St. Paul	−38.71	77.54	Poor ocean signal agreement
Juan Fernandez	−33.62	−78.83	Overlap data period too short
Easter Island	−27.15	−109.45	No reliable land motion estimate
San Felix	−26.28	−80.13	Overlap data period too short
Arica	−18.47	−70.33	No reliable land motion estimate
Cocos Island	−12.12	96.90	Possible tide gauge level shift
Callao	−12.05	−77.15	Apparent nonlinear land motion
Nuku Hiva	−8.93	−140.08	Possible tide gauge level shift
Rabaul	−4.20	152.18	Apparent nonlinear land motion
La Libertad	−2.20	−80.92	Apparent nonlinear land motion
Sao Tome	0.02	6.51	No reliable land motion estimate
Buenaventura	3.90	−77.10	Apparent nonlinear land motion
Lome	6.13	1.28	Overlap data period too short
Guam	13.43	144.65	Apparent nonlinear land motion
Socorro	18.73	−111.02	Apparent nonlinear land motion
Cabo San Lucas	22.88	−109.91	Apparent nonlinear land motion
Flores	39.45	−31.12	Poor ocean signal agreement
Basques	47.57	−59.13	Overlap data period too short
Churchill	58.78	−94.20	Overlap data period too short
Qaqortoq	60.72	−46.03	Overlap data period too short

a useful impact on the drift estimation. Second, we are now examining the nearest eight altimetric passes rather than the nearest four, as was done by M98. Thus, some stations (mainly coastal ones) where none of the nearest four passes are usable can now be included. Including these more distant altimetric series is acceptable in the present method because of the improved signal matching and cancellation we are now achieving (see below). Note, however, that the altimetric passes that are more distant from the tide gauge generally receive less weight in the final difference series, since we still weight the different pass series in a manner similar to that used in M98 when combining them into a single difference series.

In M98, no concerted effort was made to match the ocean signals in the tide gauge and altimetric series. The altimetric height series for a given pass were simply differenced from the tide gauge series using the data at a single point on the ground track. This point was taken to be at the latitude nearest that of the tide gauge. We will consider three ways in which it is likely that this could be improved. First, it is known that many of the ocean signals that we observe in the height field are propagating, and Mitchum (1994) gave an example of how this could decrease the correlation between the tide gauge and altimetric time series due to the spatial offset between the two time series. Thus, allowing for temporal lags before differencing the series should improve the signal cancellation at some stations. Second, it is not obvious that choosing the TOPEX data at the same latitude as the tide gauge is the best choice. If we allow for the possibility that the bottom topography surrounding the tide gauge may create local deformations of the large-scale sea surface height field, then it is possible that allowing for an along track spatial lag might help with signal cancellation

as well. Finally, since the tide gauge series and the altimetric series are taken at different spatial locations, it is possible that there are relatively short wavelength signals that are not coherent between the two records. Thus, in addition to allowing for temporal and spatial lags between the tide gauge and each altimetric pass examined, we also smoothed the altimetric height data slightly in the along track direction. A Gaussian set of convolution filter weights was used that passed signals at greater than 50% amplitude for wavelengths greater than approximately 90 km. The reduction in the variance of the altimetric, tide gauge difference series due to this smoothing is typically of order 10–20%. This along track smoothing improves the analysis somewhat, but it is not as important as the temporal and spatial lags. Also, the improvement is not sensitive to the details of the filter applied.

The choice of the best temporal and spatial lags is more complicated than choosing the along track smoothing width. First, each altimetric pass must be treated separately, as the distance to the tide gauge controls the temporal lag associated with the propagating signals. Second, temporal lags should be used only where the propagating signals are dominant, and this will vary from gauge to gauge. Also, the use of spatial lags depends on the topography, and must obviously be considered separately at each gauge location. Thus, the determination of the optimal temporal and spatial lags was done independently for each pair of tide gauge and altimetric pass time series. The method used is straightforward. For a given time series pair, the variance of the difference between the tide gauge series and the altimetric series was computed as a function of temporal and spatial lag. Temporal lags of up to 200 days and spatial lags of up to 4 degrees of latitude were examined, and a 2-step iteration was used to find a minimum in the variance, which is interpreted as the best signal cancellation possible. An example is shown in Figure 2, where the first step (upper panel) identifies the best lag space region as within 0–20 days in time and the best along track lag as within 50–150 km. The second step refines this to a point in lag space, which in this case is 10 days temporal lag and 90 km along track lag. In virtually all cases the temporal lags are basically consistent with Rossby wave propagation in the tropics and midlatitudes, and are typically near zero at higher latitudes. Small lags are also typical near the equator where fast wave speeds imply short temporal lags. No stations were rejected because of unreasonable lags.

After the temporal and spatial lags are determined for each of the eight passes examined for a given tide gauge, these series are combined with appropriate weighting, as discussed by M98. Several examples of the close signal matching that is now being achieved are shown in Figure 3. These stations are all from the tropical Pacific, and the improvements here are better than at many higher latitude stations, but results like these are not unusual. Rather than present a large number of examples of this sort, it is more useful to evaluate the results from the method as modified to this point to the results from the original method by M98 (Figure 4). We see immediately that the additional stations and the more careful data processing (primarily the signal matching procedure) has greatly reduced the point to point scatter in the drift estimate time series. We also note that the annual signal seen by M98 is mostly eliminated by the new processing method, and the annual amplitude in the new drift series is not statistically different from zero. Finally, note that the difference in the inferred linear drift rate between these two analyses is not primarily due to the modifications in the processing, but is from the improvement of the water vapor (TMR) correction that was briefly discussed earlier.

Estimating the Land Motion at the Tide Gauges

As stated earlier, M98 recognized that land motion at the tide gauges was an important source of systematic error in the estimation of the altimetric drift rate. No effort was made in that article, however, to carefully determine land motion rates at individual gauges, although a

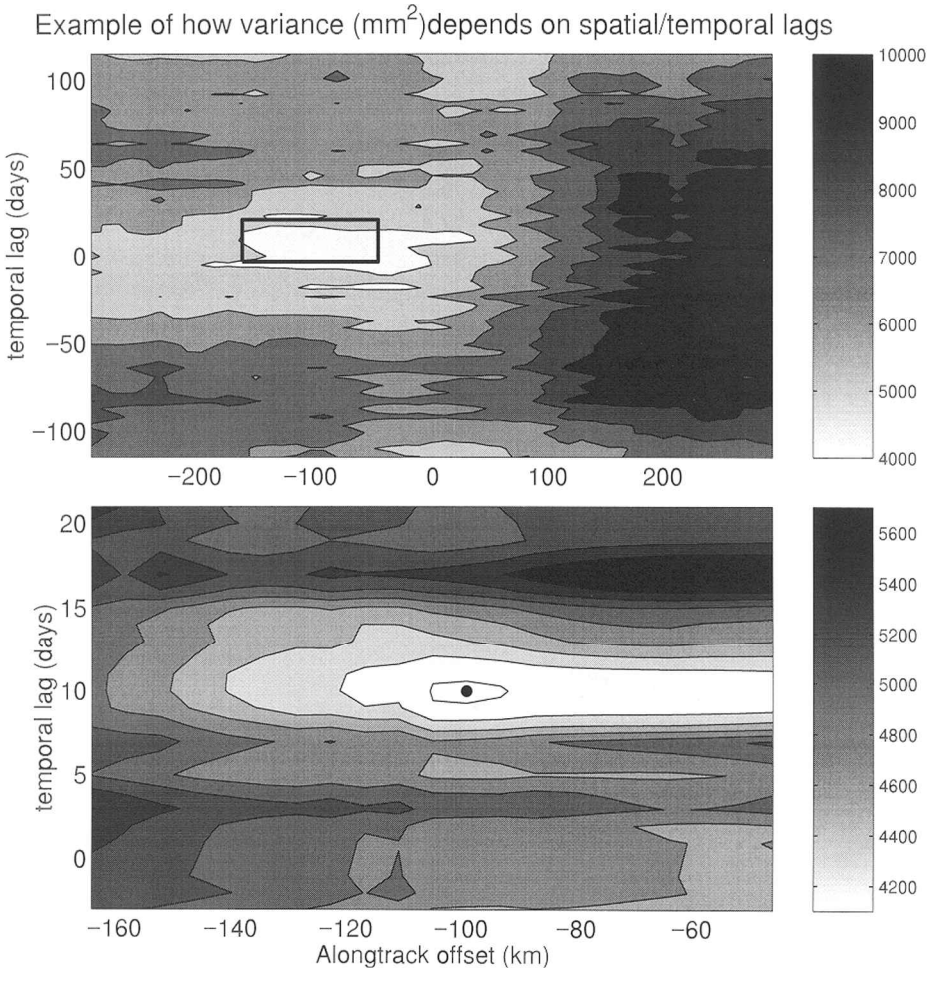

FIGURE 2 Example of how temporal and spatial lags were chosen. Each panel shows the variance of the TOPEX altimetric height, sea level difference for one tide gauge and one altimeter pass versus the temporal lag (vertical axis) and spatial lag (horizontal axis) used in matching the two time series. The spatial lag is along track, which is approximately an offset in latitude. The upper panel is from an initial iteration, and the box shown identifies the region in lag space selected for further refinement. The solid circle in the lower panel shows the final solution selected as optimal.

rough estimate of the final bias due to land motion was made, and quoted as 0.3 mm/yr with an estimated standard deviation of 1 mm/yr. This error was in fact the largest contribution to the error in the TOPEX drift estimate, and M98 pointed out the need for improvement in this area. Cazenave and others (1999) have recently made a striking demonstration of the importance of the land motion at Socorro Island in the Pacific. These authors documented an abrupt vertical motion associated with an earthquake as well a subsequent relaxation. This study is particularly interesting in that the authors used measurements from the DORIS beacon at Socorro, which give an independent estimate of the vertical land motion rate near the tide gauge, and showed that these data could account for much of the observed low frequency sea level change at the gauge. Having independent data from space-based geodetic techniques such as DORIS and GPS is ultimately the best solution to the problem

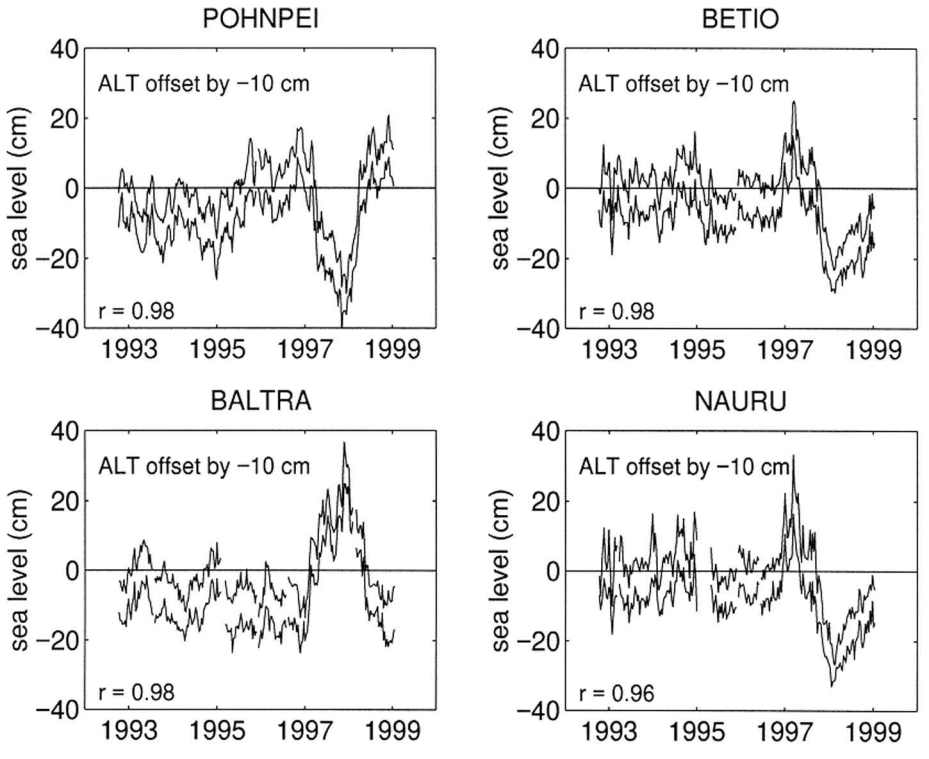

FIGURE 3 Examples of the sea level and altimetric series obtained after the spatial and temporal lags are applied. These stations are all in the tropical Pacific and illustrate some of the better, but not atypical, comparisons. The time series are sampled at one point per TOPEX cycle (about 10 days). The TOPEX heights are offset by −10 cm to aid visualization, and the correlation between the sea level and TOPEX series is indicated in the lower left corner of each subplot.

of land motion at tide gauges, and in fact a plan for satellite altimeter calibration that exploits these measurements has been presented (Mitchum 1998b). While progress has been made on this front, there are still too few GPS and DORIS measurements at present, and alternative methods must be developed for the interim. Given that researchers are already applying the T/P data to problems involving low frequency sea level change, we must make the best drift estimates possible using presently available data.

We have developed such an alternative method for the present satellite drift estimation problem. This method works by making two estimates of the land motion, which we will refer to as the internal and external estimates. The internal estimate is derived using only the sea level data from the tide gauge, while the external estimate is derived solely from the available GPS and DORIS measurements. In both cases the variances of these two land motion rates are also estimated, and the internal and external rate estimates are then combined with weights inversely proportional to these variances, which is equivalent to assuming that the internal and external rate estimates are independent. Specifically, we compute the land motion estimate as

$$\lambda_n = w_n^i \lambda_n^i + (1 - w_n^i)\lambda_n^e, \tag{1}$$

where λ_n is the land motion estimate for station n, w_n^i is the weight applied to the internal

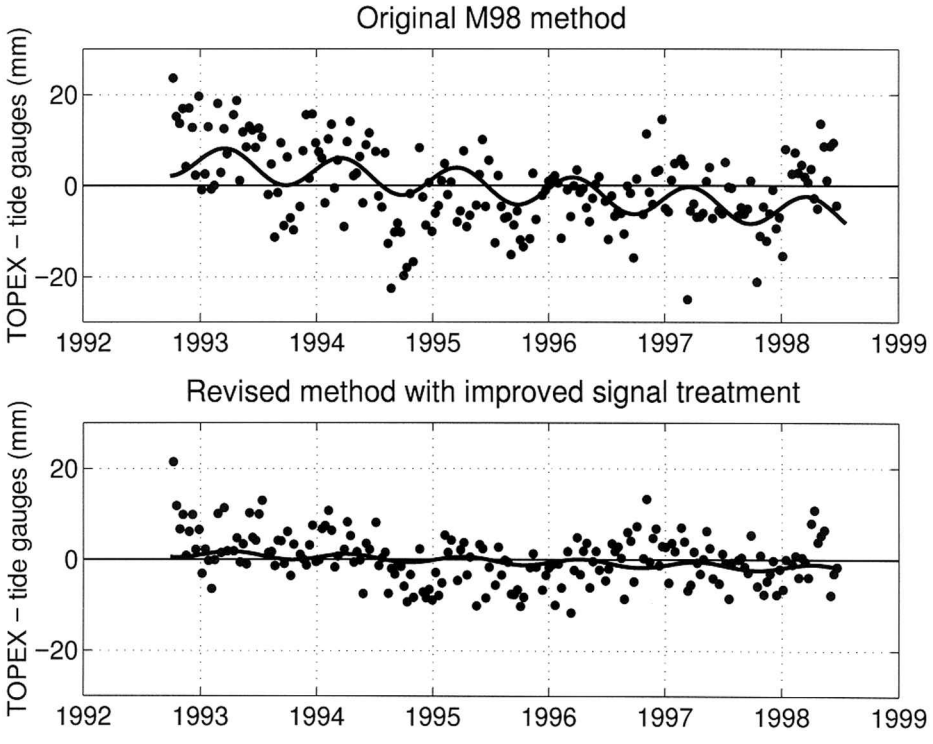

FIGURE 4 Comparison of the original M98 method (upper panel) to the present method after applying the improved signal matching algorithms (lower panel). Each solid point is one TOPEX cycle, and the solid line is a fit of an annual harmonic and a linear trend.

estimate, and λ_n^i and λ_n^e are the internal and external estimates of the land motion, respectively. The variance of λ_n is computed by standard error propagation (Beers 1962). While we realize that these land motion estimates are not ideal, our intention is to reduce the systematic error in the final drift estimate even at the possible expense of increasing the random error. Even if the land motion estimates are not highly precise, if these are unbiased, then the error in estimating trends in the TOPEX data will be reduced. That is, the systematic error is the more serious problem for the altimetric drift estimation. We reiterate, however, that the most desirable long-term solution is to make independent geodetic estimates (e.g., from GPS or DORIS) of the land motion at each tide gauge.

The basic idea behind the internal land motion estimate is to use the longest tide gauge series available at a given station to compute the long-term sea level trend, and to interpret this rate as the true globally averaged ocean sea level change rate minus the land motion rate at that station. In this calculation the monthly mean sea level time series held by the Permanent Service for Mean Sea Level (PSMSL) were used in addition to the daily time series used elsewhere in this article in order to obtain the longest series possible. No internal rate estimate was attempted for stations with less than 8 years of data. After fitting a trend to the sea level time series, we define λ_n^i via

$$\eta_{nt} = o_t - \lambda_n^i, \tag{2}$$

where η_{nt} is the observed sea level change rate, and o_t is the global average of the true oceanic sea level change rate due to long-term change in the ocean volume. This value

could in principle be obtained by averaging the rates observed by a large global set of perfect tide gauges on perfectly stable land. The error in computing λ_n^i via (2) is written schematically as

$$\epsilon_{nt} = o_{nt} + \Lambda_{nt}, \tag{3}$$

where ϵ_{nt} is the error in λ_n^i, o_{nt} is the difference between the sea level rate due to volume change at the station from the globally averaged rate, and Λ_{nt} is the apparent sea level trend due to low frequency mass redistributions (e.g., due to El Nino/Southern Oscillation (ENSO) events). The terms on the right side of (3) are discussed in detail in the following paragraphs. Once we decide how to estimate the variance associated with the various terms in (3), these can then be combined to obtain the variance estimate for λ_n^i that is necessary to apply (1) to make the final land motion estimate.

Obviously, to use (2) we must make an estimate of the true globally averaged rate in order to compute an estimate of the land motion rate. For our purposes we adopt the rate given by Douglas (1991, 1995) of 1.8 +/− 0.1 mm/yr for o_t, which was based on a careful quality control of the individual tide gauge records used to estimate the global rate and also considered land motion to some extent. It is expected, however, that the actual true rate of sea level change due to volume change at any particular tide gauge will differ from the globally averaged rate (e.g., Russell, Miller and Rind 1995) and the difference between the rate at a given tide gauge and the globally averaged rate is represented by the o_{nt} term in (3). It is difficult to estimate the magnitude of this term, but it is almost certainly larger than the standard deviation (0.1 mm/yr) for o_t given above. Note carefully, though, that the errors represented by o_{nt} are only due to true ocean volume change and not due to low frequency mass redistributions being mistakenly interpreted as volume change due to the sparse distribution of tide gauges. That error is represented by Λ_{nt}, which will be discussed shortly. For now we simply note that a bias error in our estimate of the TOPEX drift arises if the o_{nt} do not average to zero over the set of stations that we use in our analysis. If we had a truly global set, then by definition the o_{nt} will average to zero, but that is not the case for any given subset of stations. In addition to this bias error, the o_{nt} also add some random error, which is of the same order as the global rate (2 mm/yr), based on the results of Russel and others (1995).

The last error term in (3), which is denoted by Λ_{nt}, is due to the error in the sea level change rate, η_{nt} in (2), due to mass redistributions around the tide gauge being wrongly interpreted as ocean volume changes. For example, a major signal of this type that appears at many of the tide gauge locations used in this analysis is the sea level variation associated with El Nino/Southern Oscillation (ENSO) events. Other interannual to decadal signals certainly occur as well, and for finite length time series, these signals introduce significant variance into estimates of the sea level trend due to ocean volume change. In fact, the trend computed at any particular gauge typically has a value much larger than the trend due to ocean volume change, which is why attempts to use tide gauges to determine ocean volume change (e.g., Douglas 1991) must average many tide gauges and can only determine a globally averaged rate rather than regional rates. In principle, as the time series at the tide gauge becomes very long, these interannual to decadal signals will average out and the trend estimate will approach the true rate due to volume change. But given finite length series and the lack of a truly global tide gauge dataset, the Λ_{nt} will not in general average to zero. Thus we have a bias term just as for the o_{nt}, as well as a random error. The random error in this case is generally much larger than that asscoiated with the o_{nt}.

For the present purposes we combine the bias errors associated with o_{nt} and Λ_{nt} into a single term (referred to as α hereinafter) and assign it a standard deviation of 0.5 mm/yr. This

standard deviation is smaller than the errors at any particular gauge because it represents only the part that does not average to zero over the subset of gauges that we include in our analysis. This value is larger, though, than that reported by Douglas (1991, 1995). Further, we treat this error as systematic, meaning that it does not decrease due to averaging the difference series from the different tide gauges. The value of 0.5 mm/yr is uncertain, but we note that it does capture the range of published sea level change rates done using different tide gauge subsets and different estimation methods (see Douglas 1995, for a review). In addition to the bias error represented by α there is a remaining random error, which is primarily associated with the Λ_{nt} term. These random errors can be much larger than the bias errors for tide gauges with short time series, and these random errors are also probably not completely independent from gauge to gauge, being due to interannual and decadal signals that are large scale. But in general these errors are significantly smaller than the random errors in the difference time series at a given gauge due to incomplete cancellation of ocean signals and to measurement noise in the tide gauge and the altimeter. Thus, we do not expect a significant increase in the degree of spatial dependence due to the random part of the Λ_{nt} errors.

The random errors as defined above do not contribute to the more important bias error, but these errors do degrade the precision of the drift estimates, and should therefore be minimized as far as possible. Since the random errors decrease as the time series length used to fit the trend increases, we first searched for the longest possible time series at each gauge we are using. In determining the random error variance associated with Λ_{nt}, however, serial correlation in the fit residuals is carefully accounted for, which again points out the need for long time series. Another way to reduce the variance associated with the Λ_{nt} errors is to model the low frequency signals that give rise to these errors and simultaneously remove these signals when fitting the sea level trend. As mentioned above, many of the stations have variability associated with the ENSO events, although this is certainly not true at all stations. This signal was modeled by including the Southern Oscillation Index (SOI) and the Hilbert transform of the SOI as predictors when carrying out the regression that estimates the sea level trend, η_{nt}. Including the Hilbert transform of the SOI allows the model to adapt to variations in the timing of the sea level response to the ENSO events at different tide gauges. An example of the model fits obtained by including these interannual predictors is shown for the station at Pohnpei in the tropical Pacific (Figure 5). In this case, the model has succeeded in capturing much of the interannual variation, thus whitening the residual and increasing the number of degrees of freedom, or equivalently, decreasing the degree of serial correlation. Of course, the two additional parameters in the model fit reduces the number of degrees of freedom, but the variance reduction in the fit residual can be quite significant, and easily justifies the loss of 2 degrees of freedom in most cases. To give a few examples, at Pohnpei the fit residual is reduced from 73 to 45 cm^2 by including the SOI terms, while at Kapingamarangi in the western equatorial Pacific the reduction is from 62 to 43 cm^2, and at Christmas Island in the central Pacific the reduction is from 74 to 47 cm^2. Although this procedure helps at many stations, it has no effect at others, for example, at high latitudes where the ENSO signals are small compared to other low frequency signals. In the future, it may be possible to include other model functions, but we reiterate that the best long-term solution is to obtain direct geodetic estimates of the land motion at the tide gauges.

We turn now to the estimate of the external land motion rate, λ_n^e, which is based on the independent data from GPS and DORIS. For the present purposes, rates from a global set of GPS receivers were obtained from M. Watkins at the Jet Propulsion Laboratory in the United States. These rates also had associated variances, but these were formal errors that did not take into account serial correlation in the residuals. Monthly time series of DORIS data were

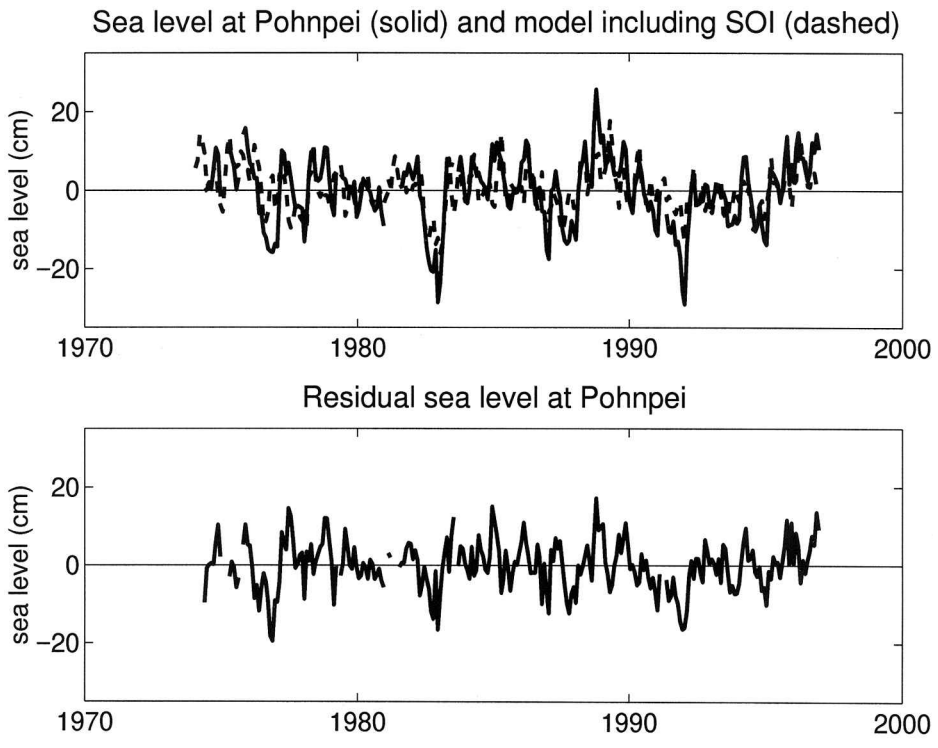

FIGURE 5 Example of the impact of including the SOI in the trend modeling necessary to estimate the internal land motion rate. In the upper panel the monthly mean sea level from Pohnpei (solid line) is shown with the fitted model (dashed line), which consists of a mean, a seasonal cycle (annual and semiannual components), the SOI, and the Hilbert transform of the SOI. The fit residual is shown in the lower panel on the same scale.

obtained from A. Cazenave at CNES in France. In order to account for the variance inflation due to serial correlation, rate fits were done for the DORIS time series, and the equivalent number of degrees of freedom was estimated by examining the autocorrelation function for the residuals. This resulted in standard deviations for the DORIS rates that were typically three times larger than the formal error estimates. In order to make better error estimates for the GPS rates, we assumed that the variance inflation factor for those series would be comparable, and therefore multiplied the provided formal standard deviations by 3. This adjustment is of a similar order, but somewhat smaller, than analogous factors recently estimated for GPS velocities by Mau, Harrison and Dixon (1999). These calculations result in a global set of geodetic (i.e., GPS and DORIS) land motion rates and associated variances that have been approximately corrected for serial correlation.

The full set of geodetic stations was reduced to the set of stations that were within 50 km of a coastline and that had standard deviations for the land motion rates less than 10 mm/yr. (Figure 6). The coverage is fairly sparse, and many tide gauge stations (see Figure 1) do not have a geodetic estimate in close proximity. In order to make a land motion estimate at the tide gauge location, all geodetic stations within 1000 km were examined, and the nearest ones (up to seven maximum) were averaged. No rate was computed if no geodetic stations were within 1000 km of the tide gauge. The averaging was done with weighting inversely proportional to the variance of the geodetic rate after this variance was multiplied by a distance factor that linearly increased the variance as the distance between the tide gauge

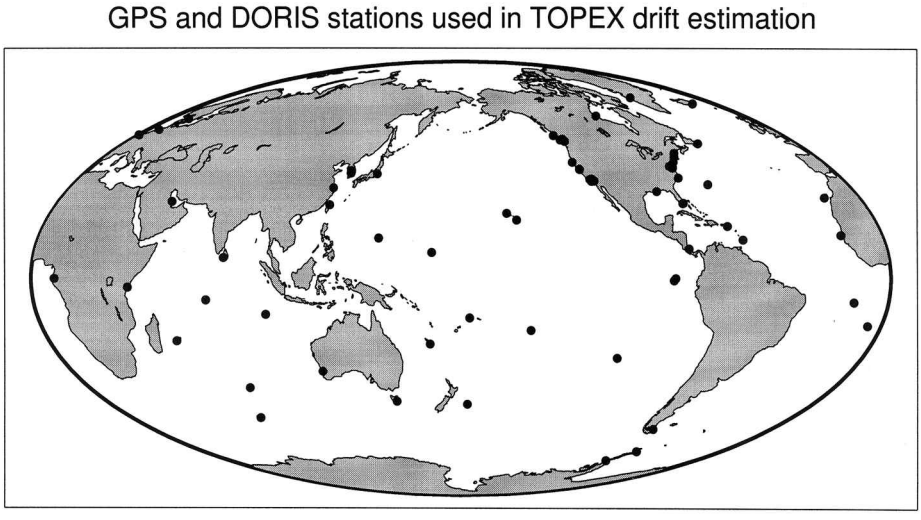

FIGURE 6 Space-based geodetic measurements used in this study. Rates are available from continuous GPS and DORIS measurements. Only stations within 50 km of a coastline and with rate standard deviations less than 10 mm/yr are used.

and the geodetic station increased. Specifically, the variance was doubled over a distance of 200 km. Thus, geodetic stations that are close to the tide gauge typically receive more weight in the averaging. Although this distance weighting system is admittedly ad hoc, it is not all obvious how to best do this weighting, and this is the topic of other work in progress. For the present, a simple calculation was done to verify that this approach had some validity. This check assumes that the internal and external rate estimates both had some skill, and thus that the pairs of rates obtained at the various tide gauges should be correlated. When this correlation is computed versus the scale for the distance weighting (Figure 7), the value of 200 km is optimal in the sense that smaller and larger values, which downweight more and less distant stations, respectively, result in decreased correlation values.

This idea that the two land motion rates should be correlated if both approaches are basically sound can again be exploited to do a simple consistency check for both estimates. We first identified 71 tide gauge stations where both rates were available. We rejected 12 stations where the rates were not well-determined, having standard deviations greater than 5 mm/yr. We also rejected eight outlier stations where the difference in the rates was greater than 3 standard deviations. This left 51 stations where we expected that the rate estimates from both methods should be reliable, and which we expected to exhibit significant correlation. We find (Figure 8) that the correlation is 0.7, which is significantly different from zero with 95% confidence even if only eight of the 51 stations can be considered independent. In fact, there is little reason to suspect substantial dependence between the stations for this calculation. This correlation is thus interpreted as a first order confirmation that our two land motion estimates are both reliable, at least in the sense that they are consistent with one another at stations where both are available.

Computation of the Drift Estimate Time Series

We are now in a position to compute the modified drift estimates at each point in the altimetric time series. Using the results from the previous section we have estimates for the land motion rate at each tide gauge, and these are used to remove a linear function from

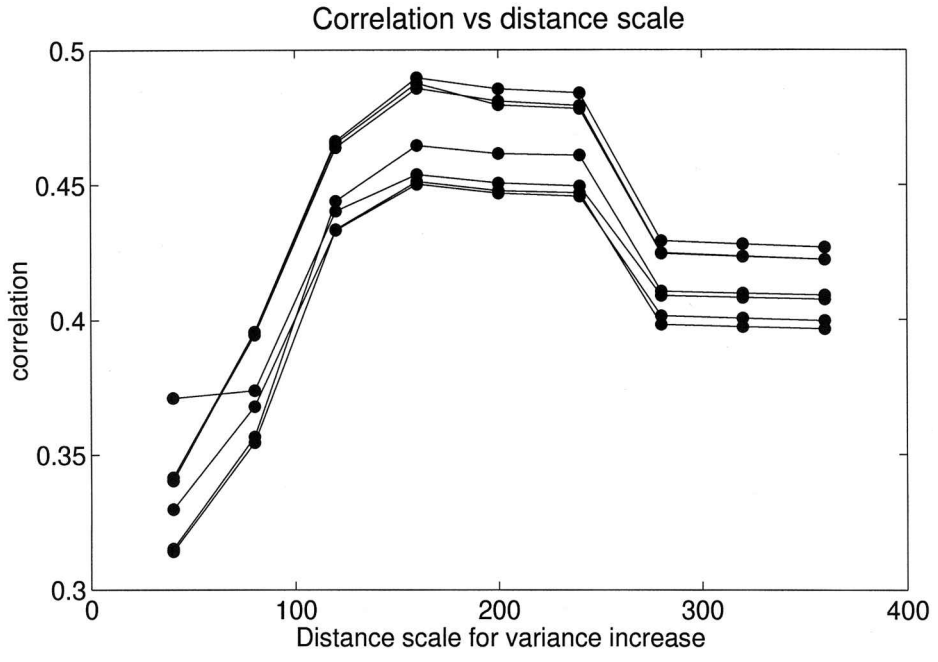

FIGURE 7 Correlation of internal and external land motion estimates versus the length used to inflate the external rate estimate variances. The external rates have variances at each site, and these are inflated with a linear function of distance with a given length scale, which was varied to make this plot. For each value of the length scale, the correlation between the averaged external rate and the internal rate at each tide gauge station is computed and plotted. The different curves are for the number of geodetic stations that are averaged at each tide gauge station, varying from 1–8. The standard deviation of the correlation under the null hypothesis of zero correlation is estimated to be approximately 0.15, so that a value of 0.3 is different from zero at the 95% confidence level.

the tide gauge sea level time series. Using the results from the section before that, we also know how to process the altimeter time series for each pass, including the temporal and spatial lags that best align the ocean signals in the altimetric and tide gauge time series. These series are then differenced, producing one measure of the altimetric drift. Recall, though, that series such as this are computed at the nearest eight passes to the tide gauges, and these series need to be combined into a single series for each tide gauge. M98 carefully considered the covariance matrix for difference series from the different passes used at a given tide gauge and for difference series from different tide gauges, and found that the most significant correlations were between the time series that resulted from differencing the time series from the multiple altimeter passes with the same tide gauge time series. This correlation was on the order of 0.2, and was attributed to serial correlation in the ocean signals in the tide gauge time series that were not removed in the difference. In the present method this correlation is taken into account by setting the correlation between the eight difference series to be 0.2, and then computing as weighted average where the weights are inversely proportional to the variance in the difference series from each pass. Taking this correlation into account does not change the weighting greatly, but it does increase the variance associated with the combined difference series. The main effect of the weighting is that passes that are further away from the tide gauge, which generally have larger differences, are thus downweighted in computing the combined difference series, as in M98.

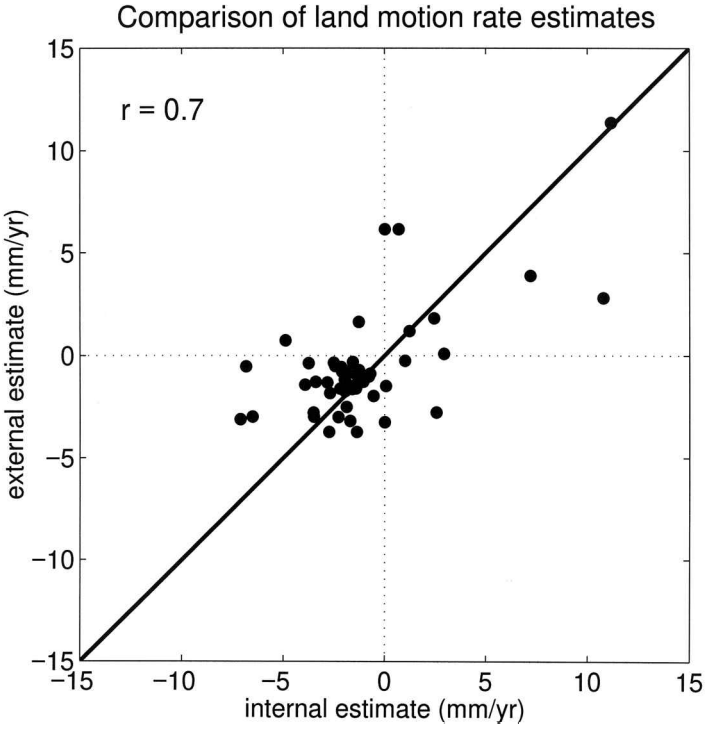

FIGURE 8 Comparison of land motion estimates from the internal and external methods that are combined to produce the final estimate at each tide gauge. Only stations where both rates are available and both are considered reliable (see text for details) are used, and 51 of the 108 stations meet these criteria. If all 51 stations are independent, a correlation of 0.3 is significantly different from 0 at the 95% confidence level. If the one point at the upper right is excluded from the fit, the correlation drops to 0.5, which is still significantly different from zero since little dependence is expected between the internal and external estimates. This correlation indicates that both the internal and external rate estimates are basically reliable, since if either were badly wrong no correlation would be expected.

Since the correlations between the different pass series at a given tide gauge have been accounted for in computing the variances for the combined difference time series at that tide gauge, and since M98 did not find significant correlations between the difference time series from separate tide gauge stations, the difference series from the available tide gauges are now considered nearly independent. We do not have complete independence, however, because of the systematic error due to the land motion correction that is still common to all of these series. It is necessary to consider this point in more detail. Schematically, for a single point in the difference series at a given station we write

$$\delta_n = \delta_n^T + \epsilon + w_n^i \alpha t, \tag{4}$$

where δ_n is the observed TOPEX, tide gauge difference at time t, δ_n^T is the true deviation that would be observed if the random and systematic errors were zero, ϵ is the random error contribution, w_n^i is the weight applied to the internal land motion estimate, α is the (unknown) error in the adopted ocean rate introduced in the section on estimating land motion, above, and t is the time relative to the center of the time series being analyzed. The last term is the systematic error, with the only contribution coming from the internal land

motion estimate (i.e., if we had geodetic information at every tide gauge, then this term would not appear). Also, while we do not know α, the error in taking the true ocean sea level change rate to be 1.8 mm/yr at every tide gauge, we have estimated its standard deviation, which we will call σ_o, to be 0.5 mm/yr. From this equation we note two things. First, we can write the standard deviation of the systematic error, which is a function of time, in terms of the weight given to the internal land motion estimate as

$$\sigma_n = w_n^i \sigma_o t, \tag{5}$$

where the standard deviation of the systematic error at this station is denoted by σ_n. Second, it is easy to verify that even for the largest t values, the variance associated with the systematic error is typically much smaller than that associated with the random error. That is, σ_n^2 is much less than the variance of δ_n. Thus, using the variance of the series itself as an estimate of the variance associated with the ϵ term, as was done in M98, is reasonable.

We now need to combine the differences at each station at a single point in time (δ_n) to obtain the final estimate of the altimeter offset at that point in time. Since the variances of the δ_n are dominated by the random errors, the deviations from the different stations are combined with weights similar to those used in M98, with the simplification that the different stations can now be considered independent since we have already accounted for the only important correlation that M98 found. Technically, the correlation due to the systematic error should also be taken into account, but it can be shown to be less than 0.01 and can, therefore, be neglected. The correlations associated with the random error in the land motion estimate (the Λ_{nt} in that section) are similarly neglected, as discussed earlier. Note that although the systematic error is not important in this context, it is essential to take it into account when fitting models (e.g., a linear trend) to the drift estimate time series, as will be discussed shortly. After combining the δ_n at each point in time we have the globally averaged difference series, Δ_t, which is computed as

$$\Delta_t = \sum w_n \delta_n, \tag{6}$$

where the w_n are the weights computed from the variances of the δ_n series. Typically we fit models to this series (e.g., M98 fit a linear trend). This is where the systematic error has to be considered very carefully. We also need, as usual, to take into account serial correlation in the drift series, but this can be done in a straightforward fashion, and we will focus instead on the systematic error here.

In order to illustrate the problem, we will write the drift series, Δ_t, as composed of a signal proportional to a set of model functions plus the random and systematic error contributions. That is, in matrix form,

$$\Delta = \mathbf{Fa} + \epsilon + \left[\alpha \sum w_n w_n^i\right]\mathbf{t}, \tag{7}$$

where Δ is the vector of drift estimates, **F** is the matrix of functions to be fit, **a** is vector of coefficients for the model functions to be determined by least squares, ϵ is the vector of random errors (which is not assumed to be free of serial correlation), and **t** is simply the vector of the time values. The variables comprising the term in the brackets are defined above in (1), (4), and (6), and together represent the net contribution of the error in estimating the true ocean sea level change rate, which is α, after weighting the internal and external land motions estimates at each station (hence the w_n^i), and doing the weighted average over all the stations (hence the w_n).

For simplicity in this presentation, we will take the ϵ vector to be uncorrelated with uniform variance, so that $\mathbf{a}'$, the fitted estimate of $\mathbf{a}$, is given by

$$\mathbf{a}' = \mathbf{a} + \mathbf{a}_\epsilon + \left[\alpha \sum w_n w_n^i\right][(\mathbf{F}^T\mathbf{F})^{-1}(\mathbf{F}^T\mathbf{t})], \tag{8}$$

where $\mathbf{F}^T$ is the transpose of $\mathbf{F}$, and $\mathbf{a}_\epsilon$ is the familiar error in $\mathbf{a}$ due to the random errors which can be treated by standard methods. The last term, on the other hand, is due to the projection of the systematic error on to the basis functions. The contribution to the variance of $\mathbf{a}$ due to this term is thus easily computed from (8) given the variance of α, which we have denoted by σ_o. The simplest illustration is the case where $\mathbf{F}$ is a vector of ones, which would be used to determine the mean value of Δ_t. In this case, the systematic error does not contribute, because there is no correlation between the basis function and the t function, which is a linear function defined to be zero at the midpoint of the time series. Another simple, but more interesting, case is where we are fitting only a trend, in which $\mathbf{F}$ is identical to $\mathbf{t}$. In this case the contribution of the systematic error to the variance of the trend estimate is written as

$$\left[\sigma_o \sum w_n w_n^i\right]^2, \tag{9}$$

and we now have an expression that quantifies the increase in the error of a linear trend estimate fitted to the drift series due to the systematic error in estimating the land motion. The systematic error contributions when fitting more complicated model functions can be derived from (8) in an analogous fashion.

Before moving on to the results from the modified drift estimation method, note that for the important case of fitting a trend, which gives the simplest estimate of the altimetric drift, we can see from (9) how to minimize the error due to the land motion error. Specifically, we need to make w_n^i small at the stations where the w_n are largest. That is, we need to obtain geodetic information at the tide gauge stations that have the best agreement with the altimeter, which leads to small variance in the difference time series at that station and hence to larger w_n values. As an example, the quantities making up the sum in (9) were computed for the 108 stations used in the present analysis of the drift and plotted versus w_n (Figure 9). The largest seven contributors to the sum (Table 2) account for 40% of the total, indicating

TABLE 2 Tide Gauge Stations Where Geodetic Information Would Make the Most Impact

Station	N Lat	E Lon	σ_e^*	$\sigma_i^\dagger$	D‡ (km)
Pohnpei	6.98	158.23	10.00	1.29	1064
Majuro	7.11	171.37	3.97	1.13	440
Christmas	1.99	−157.48	10.00	2.06	1993
Kanton	−2.81	−171.72	10.00	1.99	1262
Kwajalein	8.73	167.73	2.23	0.32	1
Pago Pago	−14.28	−170.68	4.82	0.48	605
San Juan	18.46	−66.12	1.93	0.54	180

*Standard deviation of the external land motion estimate in mm/yr. A value of 10.00 mm/yr means that no external estimate was computed.

†Standard deviation of the internal land motion estimate in mm/yr.

‡Distance in km from the tide gauge to the nearest GPS or DORIS station.

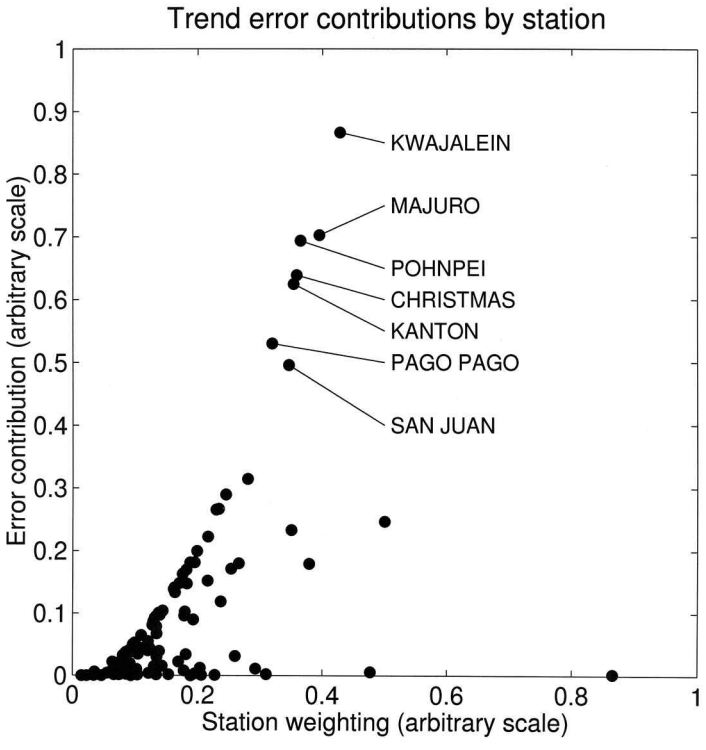

FIGURE 9 Contributions to the error in the linear trend coefficient fitted to the drift time series. The vertical axis is the contribution to the error from (9), and each solid dot is the contribution from the 108 tide gauge stations used in the analysis. The contributions are plotted versus the weight that each station receives in the global average, which accounts for the systematic increase of the contributions along the horizontal axis. The sum of these values is proportional to the total error in the linear drift coefficient, so stations that lie in the upper part of the plot are ones where geodetic information would most quickly reduce the total error. The stations with the seven largest values are identified on the figure (see also Table 2).

that attention to this relatively small set of stations would have a disproportionate impact on the overall analysis. Note that some of these stations (Pohnpei, Christmas, and Kanton) are where no geodetic information is available at all. At the other stations the available geodetic information is not adequate to outweigh the high precision of the internal land motion estimates at these stations, and therefore needs to be improved. This is even true at Kwajalein, where a GPS receiver is located just over 1 km from the tide gauge. Of course, it is possible that the error in a linear drift estimate might be better if we simply set the internal land motion estimate to zero whenever the external rate estimate was available at all. That is, we could seek to minimize the variance of the linear component of the drift estimate. This is currently being considered, but since the present drift series is not well-modeled by a linear function, it is not obviously the best approach. Again, the real long-term solution is simply to have high quality geodetic information available at as many gauges as possible. But an important result from this new approach to the calibration problem is that we now have a way to quantitatively assess which stations would benefit most from improving the geodetic estimates from GPS or DORIS receivers, at least for the purpose of calibrating satellite altimeters.

Results from the New Technique

We have already illustrated the effect of some of the changes made in the calibration method since the M98 article, which was to decrease the point-to-point noise in the estimates of the drift series (Figure 4). This decrease is mainly due to the more careful signal matching accomplished with the temporal and spatial lags incorporated before differencing the altimetric and tide gauge data. We will now evaluate the impact of the land motion estimates on our ability more carefully to detect and diagnose drifts in the altimetric series. Before comparing the modified technique to the earlier M98 results for the TOPEX data, though, we should note that there was recently a significant change in the TOPEX data used in this study.

The TOPEX portion of the T/P mission actually flew two redundant altimeters. The altimeter in use during the first 6.4 years (until 9 February 1999) of the mission is referred to as the Side A altimeter, and it became apparent during the past two years that this altimeter was drifting, an error that was attributed by the T/P project to a degradation in the point target response (PTR) characteristics of the Side A altimeter. Determining the precise drift that occurred, however, is difficult, although a retracking calculation (see Rodriguez and Martin 1994, for a discussion of retracking) for the entire Side A dataset may eventually help with this determination. For the present, we simply know that during cycle 236 (9–18 February 1999) the mission was switched to the Side B altimeter, and in addition to a possible drift error prior to that cycle, we also have an unknown vertical offest at the Side A to Side B boundary. Although the performance of the Side B altimeter has been excellent thus far, it is necessary to calibrate this (new) instrument, and in particular to independently determine the vertical offset in the heights obtained from Side A and Side B. We will first compare the present technique to the previous M98 technique using only the Side A data up to T/P cycle 235. At the end of the section we will present an estimate of the Side A to Side B offset.

The current result from the updated method discussed above (Figure 10) shows again that a primary difference is that the scatter is significantly reduced (cf., Figure 4). A quadratic model was fit to the drift series, with the errors computed with allowance for serial correlation and also for the systematic error discussed in the preceding section. The inferred linear component of the drift rate is now within 2 standard deviations of zero, but a significant quadratic trend remains. Note that the error in the new trend coefficient, which is largely due to the systematic error, is smaller than the 1.2 mm/yr error estimate made by M98, indicating that the land motion estimates have made a substantial improvement in our ability to detect linear trends despite the uncertainty in the internal land motion estimate. The error is now on the order of 0.4 mm/yr, which we take as a detection limit for the revised method. It is natural to ask how sensitive this result is to the particular set of stations that we are using in this study. To examine this question we divided the stations in two roughly equal subsets in a variety of ways, such as island versus coastal stations, northern versus southern hemisphere, Pacific versus other stations, and tropics versus outside the tropics. The linear component of the drift estimate over all of these subsets ranged from -0.34 to -0.67 mm/yr with a standard deviation that was typically 0.4 to 0.5 mm/yr, as, compared to the value of $-0.55 +/- 0.39$ mm/yr using all of the stations. Our result thus appears to be robust with respect to the specific stations included in the analysis.

The source of the quadratic component of the drift is presently unknown. It is possible that this is the signature of the PTR error mentioned above, but this is not known to be true. Another possibility that has been discussed within the T/P project is that a correction known as the internal calibration (Hayne, Hancock and Purdy 1994) is not functioning properly. This adjustment to the data is based on an internal calibration mode that makes an onboard measurement of the stability of the measurements. This estimate was only designed

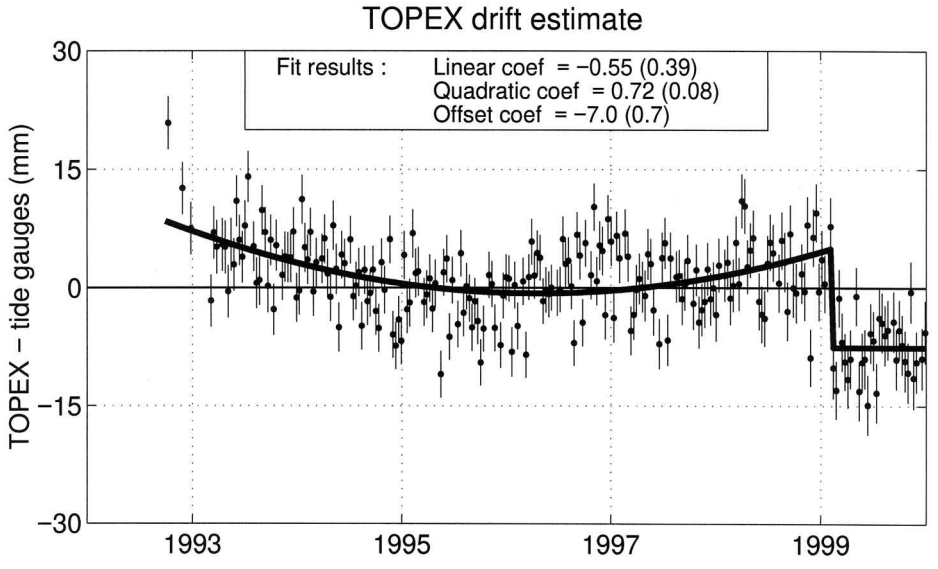

FIGURE 10 The present estimate of the TOPEX drift computed from the global tide gauge analysis using the method described in this article. The solid dots and error bars are the estimates that are computed independently for each cycle (about 10 days in duration) of the TOPEX data, and the solid line is the result of fitting a second order polynomial to the Side A data, and a constant to the Side B data. The fit takes into account serial correlation in the drift series as well as the systematic error due to the land motion correction, and the errors quoted for the fit coefficients in parentheses are one standard deviation. The offset coefficient is the difference in mm between the fitted Side B level and the mean of the Side A data after the quadratic model trend is removed.

to measure relatively large errors, however, since the precision of the T/P data has surpassed expectations. The primary reason for the suspicion about the internal calibration is that this correction has a roughly quadratic shape, and thus appears similar to the present tide gauge estimate of the altimetric drift. At this point, we do not see a compelling reason to disbelieve the internal calibration, but it should definitely be a subject for ongoing consideration, which is, of course, also true for any component of the altimetric system.

Turning to the Side A to Side B calibration, we see this as an excellent opportunity to test the tide gauge calibration method on a different type of problem. As the length of the altimetric time series increases, it is inevitable that we will need to combine data from different altimetric missions that will not always overlap temporally. Determining the vertical offsets between such missions is problematic, and if these offsets are not well-determined we will have altimetric time series with an unknown step function included. By analogy to tide gauge data, we would say that we have a datum shift. If, on the other hand, the two altimetric missions overlap, then comparing the two altimetric series during the period when both were operating would probably be more accurate. If that cannot be done, however, the tide gauge method might be our best method for leveling the two series together.

We have extended the TOPEX series past the switchover point, including data through cycle 271, which thus includes approximately 350 days of Side B data. For the extended time series (Figure 10) we model the drift series with a quadratic model for the data up to the switchover point, and with a constant afterward. The portion of the model applied to the Side B data can of course be made more complex after a longer time series has

accumulated. The offset coefficient quoted on the figure measures the offset of the Side B data from the mean of the Side A series after the quadratic trend is accounted for. The value is significantly different from zero, indicating that some additional correction is required to merge these two time series. Note, however, that the shift is small, and is of little concern to most studies that use the T/P data. Of more interest here is the uncertainty in the offset coefficient, which is on the order of 1 mm. It appears, then, that with less than one year of data we can remove datum shifts to that precision, and the precision should improve as the Side B time series increases in length.

For users of the TOPEX altimetric data who wish to use our estimate of the Side A to Side B offset, it is essential to know several additional details about the data processing. First, all of the interim (GDR) TOPEX data that were used, including the data for Side B, use the 15 mm bias necessary to make the Side A GDR data consistent with the final merged T/P (MGDR) data. Second, the internal calibration was used on all of the GDR data. The internal calibration series was reset to zero at the beginning of the Side B time series, and this offset is thus also reflected in our estimate of the Side A to Side B difference. Finally, the offset coefficient quoted (Figure 10) is the mean of the Side B data minus the mean of the Side A data after the quadratic trend has been accounted for. The offset is thus properly interpreted as the difference between the Side A data before these data were affected by the PTR error, which is consistent with the recommendation of the T/P project for investigators reporting values for the Side A to Side B offset.

Summary

An important advantage of the improved technique described here is that the scatter in the drift estimate time series is greatly reduced from the previous (M98) method. The drift series prior to the Side A to Side B boundary has a standard deviation of 6 mm, and less than 12% of the estimates exceed 10 mm in magnitude. This is important because it allows significant improvements in our ability to identify altimetric trends with more complicated structure than a simple linear trend, as well as capturing trends of relatively small amplitude with shorter time series. Obviously, this is most significant for applications that attempt to study relatively subtle low frequency trends, such as the determination of global sea level change. A less obvious example is the recent description of the global sea level change associated with the 97–98 ENSO event (Nerem et al. 1999). In this case global mean sea level was found to vary on the order of 1–2 cm with a duration of about 1–2 years. With the improved calibration afforded by the present technique we can eliminate the possibility that this interesting signal is due to an undetected systematic error in the altimetric system during the ENSO event. With the earlier (M98) method an event of this relatively small magnitude could not be unambiguously determined to be real.

In addition to the improvement in the sensitivity of the technique due to the improved ocean signal cancellation, another major change has been the addition of land motion corrections at the tide gauges. It must be noted, however, that the method developed here is still the weak link in the entire procedure, and the only real long-term solution to this problem is to have geodetic information at each tide gauge used in the analysis. The networks of continuous GPS and DORIS receivers are rapidly becoming more dense, and ultimately it may be possible directly to correct a large number of tide gauges for land motion using these independent data. In the meantime, the technique derived here should serve reasonably well, and at the least is a significant improvement over not making any correction at all for the land motions. Finally, we note that an important aspect of the technique developed here is that it is possible to quantify the impact of having geodetic information at any given tide gauge used in the analysis. Since the development of the geodetic network will take

time, and the expense is significant, having a method to decide, at least for the purposes of altimetric calibration, which gauges should be instrumented first, and to predict the impact of such installations, should be valuable for planning purposes. For example, Table 2 shows stations that might be usefully targeted for increased effort at this point.

There are several remaining questions that will be the focus of future work. First, although we find no clear evidence here that the internal calibration is problematic, it is a topic that should be periodically reviewed. This is because the low frequency nature of the internal calibration, if it were incorrect, would be very damaging to attempts to use the altimetric data for determinations of global sea level change, or for studies of the subtle signals that might be associated with decadal sea level variations. Second, we have shown that the tide gauge calibration method can provide useful estimates of TOPEX Side A to Side B offset, and these estimates need to be extended and improved. This problem is not different from that of combining any nonoverlapping altimetric time series, which will be essential as the length of the altimetric series increases and different missions must be combined into a single time series. As the TOPEX Side B series lengthens, we will have to allow for nonconstant models for the Side B drift, as we have been doing for the Side A series. Third, the present analysis indicates a remaining drift in the TOPEX data, which is quadratic rather than linear, but a drift nonetheless. It is unclear at this point whether this error is consistent with the PTR error mentioned above, and the planned retracking of the TOPEX data must be done before that can be determined. In the meantime efforts should continue to identify the source of this drift.

References

Beers, Y. 1962. *Introduction to the theory of error*. Addision-Wesley.

Cazenave, A., K. Dominh, M. Gennero, B. Ferret, and C. Brossier. 1998. Global mean sea level changes from T/P and ERS-1. *Physics and Chemistry of the Earth* 23:1069–1075.

Cazenave, A., K. Dominh, F. Ponchaut, L. Soudarin, J.-F. Cretaux, and C. Le Provost. 1999. Sea level changes from Topex-Poseidon altimetry and tide gauges, and vertical crustal motions from DORIS. *Geophys. Res. Lttrs.* 26:2077–2080.

Christensen, E., B. J. Haines, S. J. Keihm, C. S. Morris, R. A. Norman, G. H. Purcell, B. G. Williams, B. D. Wilson, G. H. Born, M. E. Parke, S. K. Gill, C. K. Shum, B. D. Tapley, R. Kolenkiewicz, and R. S. Nerum. 1994. Calibration of TOPEX/POSEIDON at Platform Harvest. *J. Geophys. Res.* 99:24465–24486.

Douglas, B. 1991. Global sea level rise. *J. Geophys. Res.* 96:6981–6992.

Douglas, B. 1995. Global sea level change: Determination and interpretation. *Rev. Geophys.* (supp.): 1425–1432.

Fu, L.-L. 2000. Ocean circulation and variability from satellite altimetry. In *Ocean Circulation and Climate*, edited by J. Church and G. Siedler. New York: Academic Press (in press).

Hayne, G. S., D. W. Hancock III, and C. L. Purdy. 1994. TOPEX Altimeter range stability estimates from calibration mode data. TOPEX/POSEIDON *Research News* 3:18–22.

Hong, B. G., W. Sturges, and A. J. Clarke. 2000. Sea level on the U.S. east coast: Decadal variability caused by open-ocean wind-curl forcing. *J. Phys. Oceanogr.* (in press).

JGR (*Journal of Geophysical Research*). 1995. TOPEX/POSEIDON: Geophysical Evaluation. Reprinted from the *Journal of Geophysical Research 99*:C12, December 15, 1994.

Keihm, S., V. Zlotnicki, C. Ruf, and B. Haines. 1998. TMR drift and scale error assessment. Technical report, Jet Propulsion Laboratory, Pasdena, CA.

Mau, A., C. G. A. Harrison, and T. H. Dixon. 1999. Noise in GPS coordinate time series. *J. Geophys. Res.* 104:2797–2816.

Minster J.-F., C. Brossier, and P. Rogel. 1995. Variations of the mean sea level from T/P data. *J. Geophys. Res.* 100:25153–25162.

Mitchum, G. T. 1994. Comparison of TOPEX sea surface heights and tide gauge sea levels. *J. Geophys. Res.* 99:24541–24553.

Mitchum, G. T. 1998a. Monitoring the stability of satellite altimeters with tide gauges. *J. Atmos. Oceanic Tech.* 15:721–730.

Mitchum, G. T. 1998b. A tide gauge network for altimeter calibration. In the Proceedings of Methods for Monitoring Sea Level: GPS and Tide Gauge Benchmark Monitoring, edited by R. Neilan and P. Woodworth. GPS Altimeter Calibration, Pasadena, CA, March, 1997.

Nerem, R. 1995. Measuring global mean sea level variations from TOPEX/POSEIDON altimeter data. *J. Geophys. Res.* 100:25135–25152.

Nerem, S., B. Haines, J. Hendricks, J.-F. Minster, G. T. Mitchum, and W. White. 1997. Improved determination of global mean sea level variations using TOPEX/POSEIDON altimeter data. *Geophys. Res. Lttrs.* 24:1331–1334.

Nerem, R., D. Chambers, E. Leuliette, G. Mitchum, and B. Giese. 1999. Variations in global mean sea level associated with the 1997–98 ENSO event. *Geophys. Res. Lttrs.* 26:3005–3009.

Nerem. R., and G. Mitchum. 2000. Sea level changes. In *Satellite Altimetry and Earth Sciences*, edited by L.-L. Fu and A. Cazenave. New York: Academic Press (in press).

Rodriguez, E., and J. Martin. 1994. Estimation of the electromagnetic bias from retracked TOPEX data. *J. Geophys. Res.* 99:24971–24980.

Russell, G., J. Miller, and D. Rind. 1995. A coupled atmosphere-ocean model for transient climate change. *Atmosphere-Ocean* 33:683–730.

Sturges, W., B. G. Hong, and A. J. Clarke. 1998. Decadal wind forcing of the North Atlantic subtropical gyre. *J. Phys. Oceanogr.* 28:659–668.

Wunsch, C., and D. Stammer. 1998. Satellite altimetry, the marine geoid, and the oceanic general circulation. *Ann. Rev. Earth Planet. Sci.* 26:219–253.